Characterisation of meteotsunami signatures in tide gauge records: a case study on the 2022 Hunga Tonga-Hunga Ha’apai eruption

Gong, Deyang

2024

Gong, D. (2024). Characterisation of meteotsunami signatures in tide gauge records: a case study on the 2022 Hunga Tonga-Hunga Ha’apai eruption. Student Research Paper, Nanyang Technological University, Singapore. https://hdl.handle.net/10356/182755

https://hdl.handle.net/10356/182755

Characterisation of meteotsunami signatures in tide gauge records: A case study on the 2022 Hunga Tonga-Hunga Ha'apai eruption

Gong Deyang
School of Civil and Environmental Engineering

Prof Adam Douglas Switzer
Elaine Tan Hui Zhi
Puah Jun Yu
Asian School of the Environment

Dr Watanabe Masashi
Dr Andrea Verolino
Earth Observatory of Singapore

Abstract - Meteotsunamis are long-wavelength, oceanic waves triggered by atmospheric pressure disturbances. Understanding meteotsunamis is crucial since they can potentially damage coastal infrastructure and endanger public safety as demonstrated at Dayyer, Persian Gulf in Iran on 19 March 2017, which killed 5 people and left 22 injured. Despite its importance, the characteristics of meteotsunami are not very well explored due to the scarcity of events and short instrumentation duration. Hence, part of this research project aims to address the research gap by investigating the occurrence of meteotsunami from the 15 January 2022 eruption of Hunga Tonga–Hunga Ha'apai, a submarine volcano in the Kingdom of Tonga, through analysing tide gauge records. We will analyse tide gauge data, which measures the variation in sea level over time at a specific location near east Australia. Fast Fourier Transform (FFT) is applied to the tide gauge data before and after the eruption respectively with different time durations with a focus on the 1-day and 3-day period to identify patterns that could be characteristic of meteotsunami. After which, this research will extend its FFT analysis to filter additional tide gauges in prominent port cities like Singapore and Hong Kong which have no historical record of a meteotsunami. Ultimately, the research findings could be used to assist in the improvement of coastal safety and disaster preparedness such as the development of effective early warning systems, thus enhancing the Southeast Asia and East Asia regions' abilities to anticipate and mitigate the impacts of meteotsunamis along coastal areas.

Keywords - Meteotsunamis, Hunga Tonga-Hunga Ha'apai Volcano Eruption, Tide Gauges, Fast Fourier Transform, Disaster Preparedness

1 INTRODUCTION

Meteotsunamis, so-called meteorological tsunamis, are long-wavelength, oceanic waves triggered by atmospheric pressure disturbances (Monserrat et al., 2006). They can be found in shallow seas all around the world with periods ranging from a few minutes to several hours, and in extreme cases, they can reach heights of several meters (Pellikka et al., 2020).

Historical incidents of meteotsunamis show its risk of endangering public safety and coastal infrastructure. As demonstrated at Dayyer, Persian Gulf in Iran on 19 March 2017, 5 people were killed and 22 more were left injured by meteotsunamis which caused a wave to inundate around 100 kilometers of the gulf coastline (Kazeminezhad et al., 2020). Another catastrophic example of meteotsunamis was on 3 August 2007 at Mostaganem in Algeria where 12 people were killed by an unexpected run-up of 7 to 10 meters (Okal, 2020).

Thus, understanding meteotsunamis is crucial since they can potentially result in destructive damage in the coastal area despite the scarcity of events and short instrumentation duration.

Although it is an important phenomenon, the characteristics of meteotsunamis are not well explored. Since meteotsunamis' features are nearly identical to seismic tsunamis, identifying meteotsunamis can be difficult. Moreover, meteotsunamis might be mistaken for storm surges which are caused by the wind and normal seiche activity as well (Bailey et al., 2014). Besides, Lewis et al. (2023) claimed that there is no standardised methodology for meteotsunami identification. Due to the numerous uncertainties, it is now challenging to forecast meteotsunamis events and alert the public (Bailey et al., 2014).

Moreover, in the worldwide oceans, meteotsunamis excited by volcano explosions could significantly harm the coastal infrastructure, capsize vessels in harbours, and result in a high death toll at multiple sites along the coast that are distant from the epicentre of a catastrophic event (Denamiel et al., 2023). Hence, this research project aims to partially address the research gap in meteotsunamis characterisation by specially analysing tide gauge records using Fast Fourier Transform (FFT) to identify signatures of meteotsunami that originated from volcanic events.

Tide gauge is one part of a modern water level monitoring station, and it is equipped with sensors to measure the variation in sea level over time (NOAA, 2023). Fast Fourier Transform (FFT) is an algorithm to convert a signal into a representation in the frequency domain from its original domain, which is often time or space (Heideman et al., 1984).

In this research study, a case study is conducted on investigating the characteristics of meteotsunami generated after the eruption of Hunga Tonga–Hunga Ha'apai, which is a submarine volcano in the Kingdom of Tonga (Villalonga et al., 2023; Bennis & Sennert, 2022). At 04:15 UTC on January 15, 2022, a violent eruption produced noticeable perturbations that propagated far from the source and were felt for several days after the eruption in remote places of the world in both the atmosphere and the ocean (USGS, n.d.; Villalonga et al., 2023). The generated global atmospheric and oceanic response was captured by an unprecedented number of sensors (Villalonga et al., 2023), which provided substantial data for the case study.

To proceed with research analysis, several water level monitoring stations around the Pacific Ocean with a focus near east Australia have been selected to be further examined. This will be explained further in the methodology section later.

Ultimately, the research findings could be used to assist in the improvement of coastal safety and disaster preparedness such as the development of effective early warning systems. Findings from this research could also be extended to possible future studies on the historical tide gauge records such as Singapore or Hong Kong to identify similar historical meteotsunamis events, thus enhancing the Southeast Asia and East Asia regions' abilities to anticipate and mitigate the impacts of meteotsunamis along coastal areas.

2 METHODOLOGY

The methodology includes a comprehensive literature review to establish a foundational understanding of meteotsunamis, the collection of relevant tide gauge data, and a detailed analysis of the collected data, ensuring a thorough investigation and accurate results.

2.1 LITERATURE REVIEW

To identify existing characteristics of meteotsunamis, a literature review was conducted. Reviewing literature aids the author in understanding the background and nature of the subject (Auraria Library, 2024), thus providing a foundation for understanding the criteria and patterns previously identified as associated with meteotsunamis.

2.2 DATA COLLECTION

Two tide gauges located near east Australia were selected to provide relatively high-resolution tide gauge records for this research. Records were extracted within a short period from 10 January 2022 00:00 to 20 January 2022 23:45, which started 5 days before the violent eruption and ended 5 days after the eruption, to ensure the dataset is complete and contains no missing data.

One of the tide gauge data was extracted from the National Data Buoy Center (NDBC) website. This tide gauge station has an identification number as Station 55023 and is located at 14°42'53" S 153°32'14" E, which is around 870km northeast of Townsville in Coral Sea 2. The water column height at Station 55023 usually has a 15-minute interval, with 1-minute and 15-second intervals available when significant changes are identified for water depth (NDBC, n.d.).

The other tide gauge data was extracted from an open-source dataset (Davies, 2024) under Geoscience Australia of Australia Government (GA.gov, n.d.). It has an identification number as Station 240402 and is named as Lord Howe Island Station, located at a longitude of 159.05815 and a latitude of -31.523638. These records have a 1-minute interval. Data attribution for Station 240402 is given to Manly Hydraulics Laboratory under the New South Wales Department of Planning and Environment (MHL, n.d.).

2.3 DATA ANALYSIS

The following 3 methods as resampling, high-pass filtering and Fast Fourier Transform (FFT) have been applied sequentially to analyse the collected tide gauge records.

2.3.1 Resampling

Due to the differences in the records' time interval from the two stations, resampling was applied to respective tide gauge data to change the time interval. Down-sampling was applied to Station 240402 to change its original 1-minute interval records to 5-minute intervals and 15-minute intervals. Up-sampling (or over-sampling) using linear interpolation and down-sampling were applied to Station 55023, changing its original 1-minute and 15-minute intervals to 1-minute, 5-minute and 15-minute intervals respectively.

By adjusting the time intervals, we can ensure that the data is consistent, making it easier to identify and analyse patterns over different temporal resolutions. Thus, a clearer comparison could be made when directly analysing the sea level observance plot.

2.3.2 High-pass filtering

A High-pass filter was applied to filter sea level data with a wave period of less than 3 hours. This process filters out the tidal pattern, allowing us to check the wave height with a focus on the higher frequency components of the sea level data. Since tsunamis frequently dominate short-period waves and studies typically utilise similar high-pass filters to evaluate their impacts (Davies et al., 2024), the identified 3 hours are acquired.

2.3.3 Fast Fourier Transform (FFT)

Fast Fourier Transform (FFT) was applied to the tide gauge data to transform it from the time domain to the frequency domain. Two types of Fast Fourier Transform (FFT) plots were created based on different time ranges selected. One set of plots compared the sea level frequencies for the day before the violent eruption (14 January 2022 00:00 to 15 January 2022 00:00), the day of the violent eruption (15 January 2022 00:00 to 16 January 2022 00:00), and the day after the violent eruption (16 January 2022 00:00 to 17 January 2022 00:00). The other set of plots compared the sea level frequencies for 5 days before the violent eruption (10 January 2022 00:00 to 15 January 2022 00:00) and 5 days after the violent eruption (15 January 2022 00:00 to 20 January 2022 00:00).

This method helps identify the dominant frequencies presented in the sea level data. By analysing these frequencies, possible frequency patterns for meteotsunami originating from volcanic events could be identified.

3 RESULTS AND DISCUSSIONS

In this section, the literature review findings would be introduced at the start, followed by the sea level data observance, wave height analysis, and frequency analysis with Fast Fourier Transform (FFT) result would be presented at last.

3.1 EXISTING CHARACTERISTICS OF METEOTSUNAMIS

As claimed by Pellikka et al. (2020), there is no universal criteria or definition for what qualifies as a meteotsunami, which is because nearly all variations in sea level within the tsunami frequency range are inside of atmospheric origin as well.

However, one recent research conducted by Lewis et al. (2023) has summarised the criterion to be used for sea level identification of meteotsunami as shown below:

a. Sea level disturbance periods vary from 2 to 120 minutes.

b. Wave heights surpass 0.20 meters.

c. Two or more locations or tidal gauge stations record a wave disturbance (Williams et al., 2021; Kim et al., 2021).

In this study, this criterion (Lewis et al., 2023) was used as a primary indication of whether the result findings match the previous identified meteotsunami characteristics or not.

3.2 DIRECT SEA LEVEL OBSERVANCE

Figures 1 and 2 show the tide gauge chart for Stations 55023 and 240402 recorded at different intervals respectively.

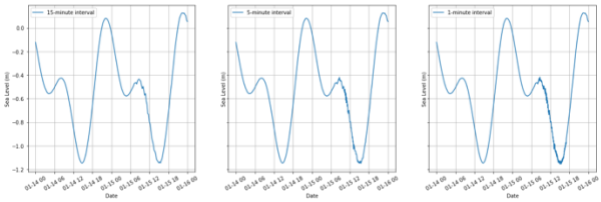

Figure 1 Sea level against time from 14 Jan 2022 00:00 to 16 Jan 2022 00:00 for Station 55023 with different record intervals (left to right: 15-minute, 5-minute, 1 minute).

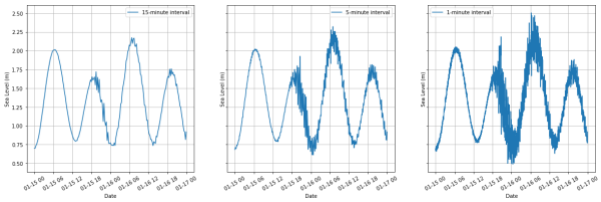

Figure 2 Sea level against time from 14 Jan 2022 00:00 to 16 Jan 2022 00:00 for Station 240402 with different records intervals (left to right: 15-minute, 5-minute, 1 minute).

Figures 1 and 2 are evident that some sea level variations can be detected in the 15-minute interval plots. However, these variations are less pronounced compared to those observed in the 1-minute interval plots.

Specifically, Figure 2 highlights a notable disturbance in sea level with a 1-minute interval, while the recorded sea level disturbance dropped by approximately 0.5 meters in the 15-minute interval data.

This suggests that while 15-minute interval data can capture mild variations as a potential indication of meteotsunamis, the significance and resolution of these variations are diminished compared to the 1-minute interval data. Consequently, the finer resolution as 1-minute data is more effective in identifying and analyzing significant sea level disturbances which may associated with meteotsunamis.

3.3 WAVE HEIGHT ANALYSIS

Figures 3 and 4 display the high-pass filtered sea level data which represented wave height without

the tidal pattern against time for Stations 55023 and 240402 respectively.

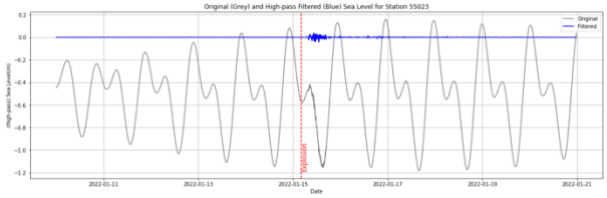

Figure 3 High pass filtered (Blue) and original (Grey) sea level against time for Station 55023, with an indication showing the time of violent eruption (Dotted Red).

From Figure 3, a mild variation in wave height could be identified, indicating the generation of a wave with a height less than 0.1 meters. However, according to the existing meteotsunami criterion (Lewis et al., 2023), a wave height exceeding 0.2 meters may be classified as a meteotsunami. Therefore, the data from Station 55023 likely captured a small sea level disturbance rather than a meteotsunami wave.

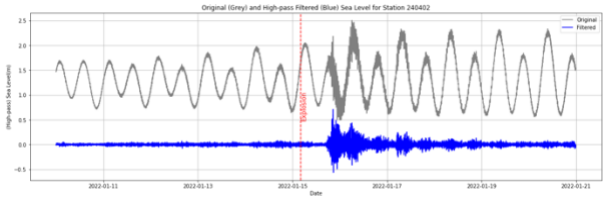

Figure 4 High pass filtered (Blue) and original (Grey) sea level against time for Station 240402, with an indication showing the time of violent eruption (Dotted Red).

In contrast, Figure 4 reveals significant variations in wave height, indicating a wave exceeding 0.5 meters, which surpasses the 0.2-meter threshold. This suggests that the wave identified at Station 240402 could potentially be generated by a meteotsunami.

Furthermore, the comparison between Figures 3 and 4 indicates that the wave at Station 240402 arrived later than at Station 55023. The underlying cause of this delayed arrival necessitates further investigation.

3.4 FREQUENCY ANALYSIS

In this section, an example of the FFT result analysis would be introduced first, followed by a summary of the FFT results and frequency analysis.

Figures 5 to 8 show FFT plots comparing sea level frequencies for the day before, the day of, and the day after the violent eruption at Station 55023 with different record intervals.

From Figure 5 using 1-minute record intervals, 2 prominent frequency peaks can be identified on the day of the violent eruption. Peak 1 at 100 to 200 cycles per day (7.2 to 14.4 minutes) and Peak 2 at 300 to 400 cycles per day (3.6 to 4.8 minutes). These peaks indicate an increase in wave activity within these frequency ranges on the day of the eruption compared to the other days. This suggests that these frequency ranges are associated with the small sea level disturbances that may be generated by the violent eruption.

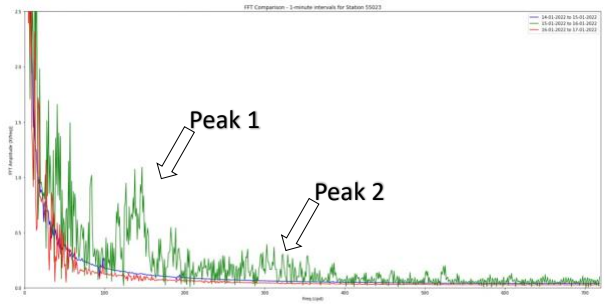

Figure 5 FFT plot comparing sea level frequencies for the day before (Blue), the day of (Green), and the day after (Red) the violent eruption for Station 55023, recorded at 1-minute intervals. 2 significant frequency peaks are indicated.

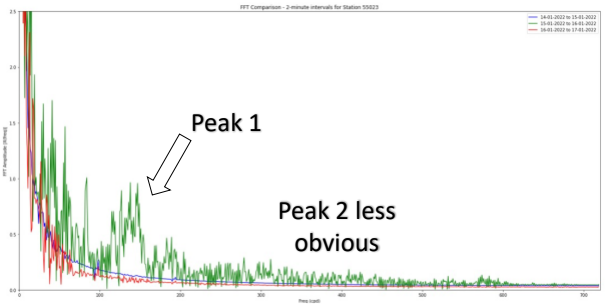

Figure 6 FFT plot comparing sea level frequencies for the day before (Blue), the day of (Green), and the day after (Red) the violent eruption for Station 55023, recorded at 2-minute intervals. 2 frequency peaks are indicated.

As shown in Figure 6 using 2-minute record intervals, Peak 2 identified in the previous Figure 5 (1-minute interval) becomes less obvious.

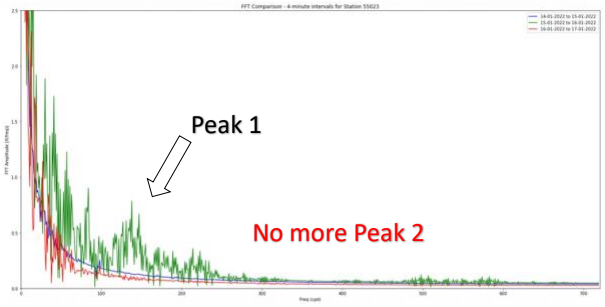

Figure 7 FFT plot comparing sea level frequencies for the day before (Blue), the day of (Green), and the day after (Red) the violent eruption for Station 55023, recorded at 4-minute intervals. 1 frequency peak is indicated.

From Figure 7 using 4-minute record intervals, Peak 2 identified in the previous Figure 5 (1-minute interval) is no longer discernible. This indicates that the maximum detectable time interval for capturing Peak 2 is 3 minutes. Beyond a 3-minute interval,

some of the frequency patterns associated with sea level disturbances may be lost.

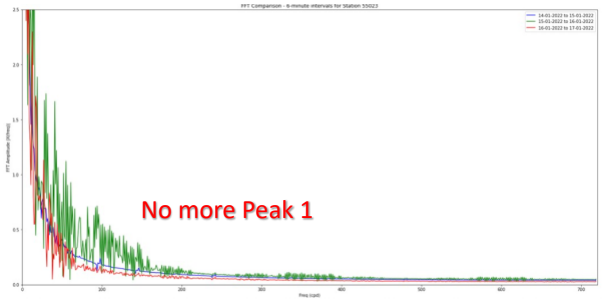

Figure 8 FFT plot comparing sea level frequencies for the day before (Blue), the day of (Green), and the day after (Red) the violent eruption for Station 55023, recorded at 6-minute intervals.

Similarly, from Figure 8 using 6-minute record intervals, Peak 1 identified in the previous Figure 5 (1-minute interval) is no longer discernible. This indicates that the maximum detectable time interval for capturing Peak 1 is 5 minutes. Beyond a 5-minute interval, all the frequency patterns associated with sea level disturbances may be lost.

Similar analysis and comparison were made to other FFT results, the summarised results are shown in Table 1 below.

Table 1 Summary of Fast Fourier Transform (FFT) Results and Frequency Analysis

Station ID	Day(s) Selected	Peak No.	Frequency Range (min)	Maximum Detectable Time Interval (min)
55023	1	1	7.2 - 14.4	5
		2	3.6 - 4.8	3
	5	1	7.2 - 14.4	5
		2	4.1 - 5.3	1
240402	1	1	9.6 - 28.8	15
		2	3.6 - 5.8	2
	5	1	9.6 - 28.8	11
		2	3.6 - 5.8	3

Based on Table 1, a 15-minute data interval may be sufficient to partially capture the possible meteotsunami pattern for Station 240402, particularly with a frequency peak (Peak 1) in the range of 9.6 to 28.8 minutes. However, data intervals from 2 minutes onwards may lose some of the frequency patterns, especially those in the range of 3.6 to 5.8 minutes (Peak 2). Therefore, while a 15-minute interval might be adequate for identifying a meteotsunami event, having 1-minute interval data would be ideal for more precise detection.

Comparisons over both daily and weekly intervals can effectively identify the frequency peaks that may represent small sea level disturbances or possible meteotsunamis. Consequently, when filtering the data, any method that simplifies the filtering process can be employed.

4 CONCLUSION

In summary, this research project investigated the characteristics of meteotsunamis generated by the 15 January 2022 eruption of the Hunga Tonga-Hunga Ha'apai by analysing tide gauge data near east Australia.

Fast Fourier Transform (FFT) applied to the tide gauge records before and after the violent eruption revealed significant frequency peaks associated with the sea level disturbances. Notably, the 1-minute interval data was more effective in identifying the fine details of these disturbances compared to the 15-minute interval data.

The findings suggest that the wave heights and frequency ranges observed at Station 240402 align with the criteria for meteotsunamis, although further verification with additional tide gauge data is necessary. At Station 240402, it captured a wave height exceeding 0.5 meters after the violent eruption and the identified 2 major peaks of frequency range lie in 3.6 to 5.8 minutes and 9.6 to 28.8 minutes.

Future research could include more tide gauges from other regions, such as Singapore and Hong Kong, to help identify possible historical events, enhancing the regional understanding of meteotsunami risks.

ACKNOWLEDGMENT

I would like to acknowledge the funding support from Nanyang Technological University – URECA Undergraduate Research Programme for this research project.

I would also like to express my sincere gratitude to Prof Adam Douglas Switzer for providing me with the opportunity to undertake this research project and supervising me. I am truly thankful to my mentors, Elaine Tan Hui Zhi, Puah Jun Yu, Dr Watanabe Masashi, and Dr Andrea Verolino for guiding and supporting me.

REFERENCES

Auraria Library. (2024, February 29). *Research Methods: Literature Reviews*. https://guides.auraria.edu/researchmethods

Bailey, K., DiVeglio, C., & Welty, A. (2014). An examination of the June 2013 East Coast meteotsunami captured by NOAA observing systems. In *NOAA.Gov.* (NOAA Technical

Report NOS CO-OPS 079). National Oceanic and Atmospheric Administration. http://tidesandcurrents.noaa.gov/publications/NOS_COOPS_079.pdf

Bennis, K. L., & Sennert, S. (2022). Report on Hunga Tonga-Hunga Ha'apai (Tonga) — 12 January-18 January 2022. In *Global Volcanism Program, 2022*. Smithsonian Institution and US Geological Survey. https://volcano.si.edu/ShowReport.cfm?doi=10.5479/si.GVP.WVAR20220112-243040

Davies, G. (2024). *GeoscienceAustralia / ptha [Data set]*. GitHub. https://github.com/GeoscienceAustralia/ptha

Davies, G., Wilson, K., Hague, B., Greenslade, D., Metters, D., Boswood, P., Maddox, S., Dakin, S. K., Palmer, K., Galton-Fenzi, B., French, J., & Kain, C. (2024). Australian atmospheric pressure and sea level data during the 2022 Hunga-Tonga Hunga-Ha'apai volcano tsunami. *Scientific Data*, *11*(1). https://doi.org/10.1038/s41597-024-02949-2

Denamiel, C., Vasylkevych, S., Žagar, N., Zemunik, P., & Vilibić, I. (2023). Destructive Potential of Planetary Meteotsunami Waves beyond the Hunga Tonga–Hunga Ha'apai Volcano Eruption. *Bulletin of the American Meteorological Society*, *104*(1), E178–E191. https://doi.org/10.1175/bams-d-22-0164.1

GA.gov. (n.d.). *Geoscience Australia - Australia Government official website*. Geoscience Australia. Retrieved June 24, 2024, from https://www.ga.gov.au/

Heideman, M., Johnson, D., & Burrus, C. (1984). Gauss and the history of the fast fourier transform. *IEEE ASSP Magazine*, *1*(4), 14–21. https://doi.org/10.1109/massp.1984.1162257

Kazeminezhad, M. H., Vilibić, I., Denamiel, C., Ghafarian, P., & Negah, S. (2020). Weather radar and ancillary observations of the convective system causing the northern Persian Gulf meteotsunami on 19 March 2017. *Natural Hazards*, *106*(2), 1747–1769. https://doi.org/10.1007/s11069-020-04208-0

Kim, M. S., Woo, S. B., Eom, H., & You, S. H. (2021). Occurrence of pressure-forced meteotsunami events in the eastern Yellow Sea during 2010–2019. *Natural Hazards and Earth System Sciences*, *21*(11), 3323–3337. https://doi.org/10.5194/nhess-21-3323-2021

Lewis, C., Smyth, T., Williams, D., Neumann, J., & Cloke, H. (2023). Meteotsunami in the United Kingdom: the hidden hazard. *Natural Hazards and Earth System Sciences*, *23*(7), 2531–2546. https://doi.org/10.5194/nhess-23-2531-2023

MHL. (n.d.). *MHL: Lord Howe Island (Live)(240402)*. Manly Hydraulics Laboratory. Retrieved June 24, 2024, from https://www.mhl.nsw.gov.au/Station-240402

Monserrat, S., Vilibić, I., & Rabinovich, A. B. (2006). Meteotsunamis: atmospherically induced destructive ocean waves in the tsunami frequency band. *Natural Hazards and Earth System Sciences*, *6*(6), 1035–1051. https://doi.org/10.5194/nhess-6-1035-2006

NDBC. (n.d.). *Station 55023 - Coral Sea 2 - 870km NE of Townsville*. National Data Buoy Center (NDBC) - National Oceanic and Atmospheric Administration. Retrieved June 24, 2024, from https://www.ndbc.noaa.gov/station_page.php?station=55023

NOAA. (2023, January 20). *What is a tide gauge?* National Ocean Service. https://oceanservice.noaa.gov/facts/tide-gauge.html#:~:text=A%20tide%20gauge%2C%20which%20is,and%20habitat%20restoration%20and%20preservation.

Okal, E. A. (2020). On the possibility of seismic recording of meteotsunamis. *Natural Hazards*, *106*(2), 1125–1147. https://doi.org/10.1007/s11069-020-04146-x

Pellikka, H., Laurila, T. K., Boman, H., Karjalainen, A., Björkqvist, J. V., & Kahma, K. K. (2020). Meteotsunami occurrence in the Gulf of Finland over the past century. *Natural Hazards and Earth System Sciences*, *20*(9), 2535–2546. https://doi.org/10.5194/nhess-20-2535-2020

USGS. (n.d.). *M 5.8 Volcanic Eruption - 68 km NNW of Nuku'alofa, Tonga*. U.S. Geological Survey - Earthquake Hazards Program. Retrieved June 24, 2024, from https://earthquake.usgs.gov/earthquakes/eventpage/pt22015050/executive

Villalonga, J., Amores, N., Monserrat, S., Marcos, M., Gomis, D., & Jordà, G. (2023). Observational study of the heterogeneous global meteotsunami generated after the Hunga Tonga–Hunga Ha'apai Volcano eruption. *Scientific Reports*, *13*(1). https://doi.org/10.1038/s41598-023-35800-6

Williams, D. A., Schultz, D. M., Horsburgh, K. J., & Hughes, C. W. (2021). An 8-yr Meteotsunami Climatology across Northwest Europe: 2010–17. *Journal of Physical Oceanography*, *51*(4), 1145–1161. https://doi.org/10.1175/jpo-d-20-0175.1

APPENDIX

The appendix contains the full set of FFT results to compare sea level frequencies before and after the violent eruption of Hunga Tonga-Hunga Ha'apai with different time intervals from 1-minute to 15-minute of the tide gauge records. These FFT results support the main findings for the frequency analysis discussed in the paper.

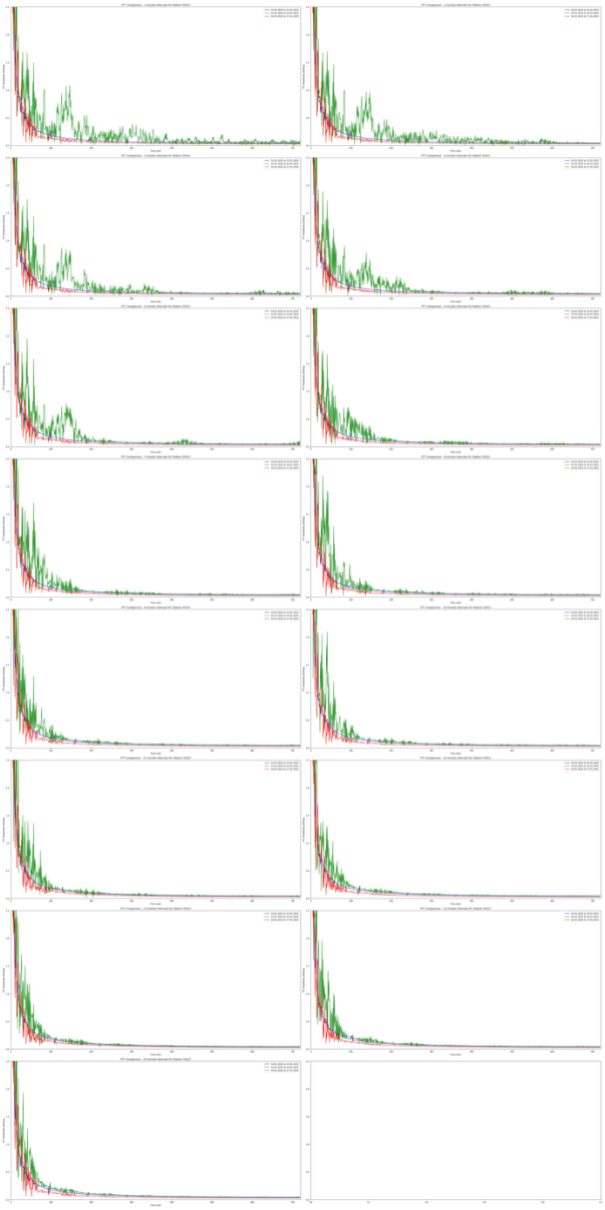

Figure 9 FFT plots comparing sea level frequencies for the day before (Blue), the day of (Green), and the day after (Red) the violent eruption for Station 55023, recorded from 1-minute to 15-minute intervals.

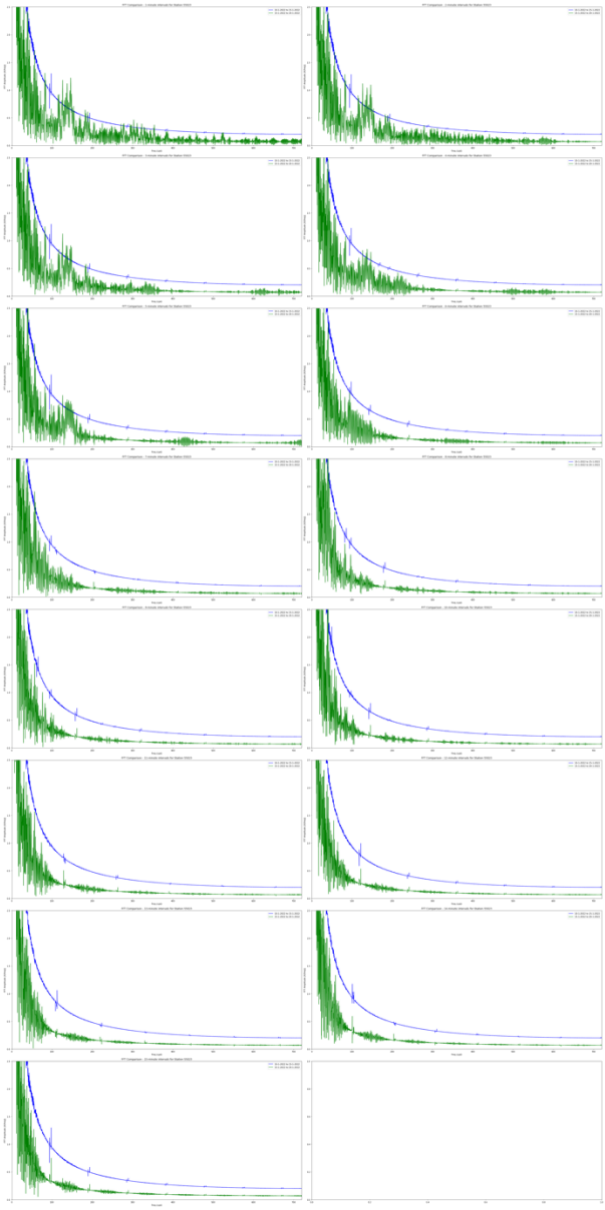

Figure 10 FFT plots comparing sea level frequencies for 5 days before (Blue), 5 days after (Green) the violent eruption for Station 55023, recorded from 1-minute to 15-minute intervals.

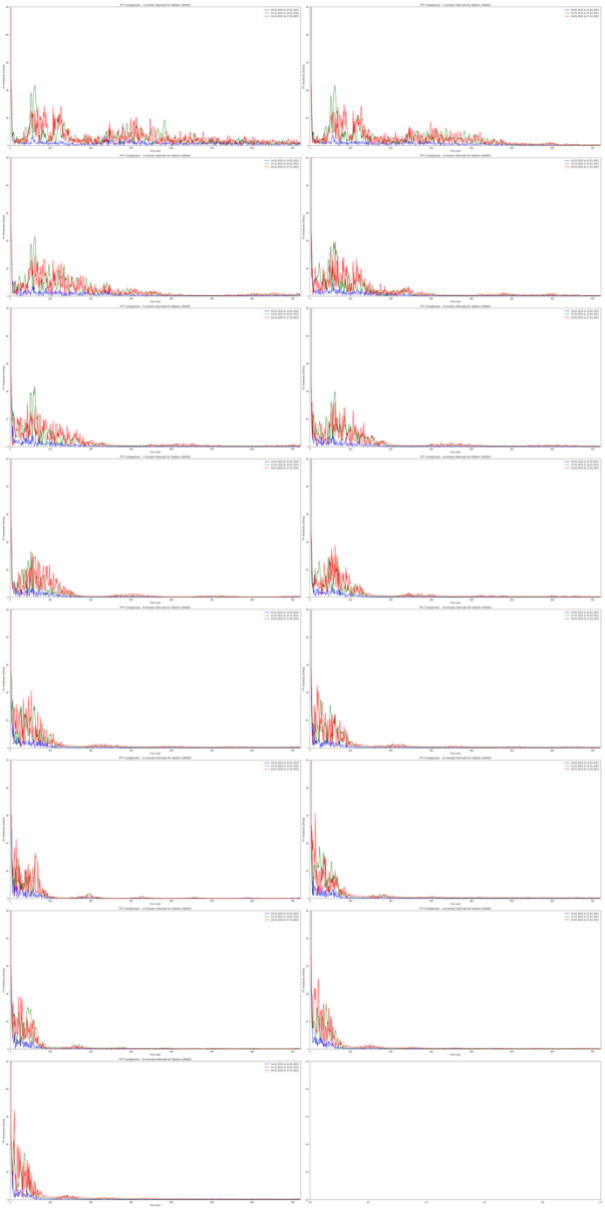

Figure 11 FFT plots comparing sea level frequencies for the day before (Blue), the day of (Green), and the day after (Red) the violent eruption for Station 240402, recorded from 1-minute to 15-minute intervals.

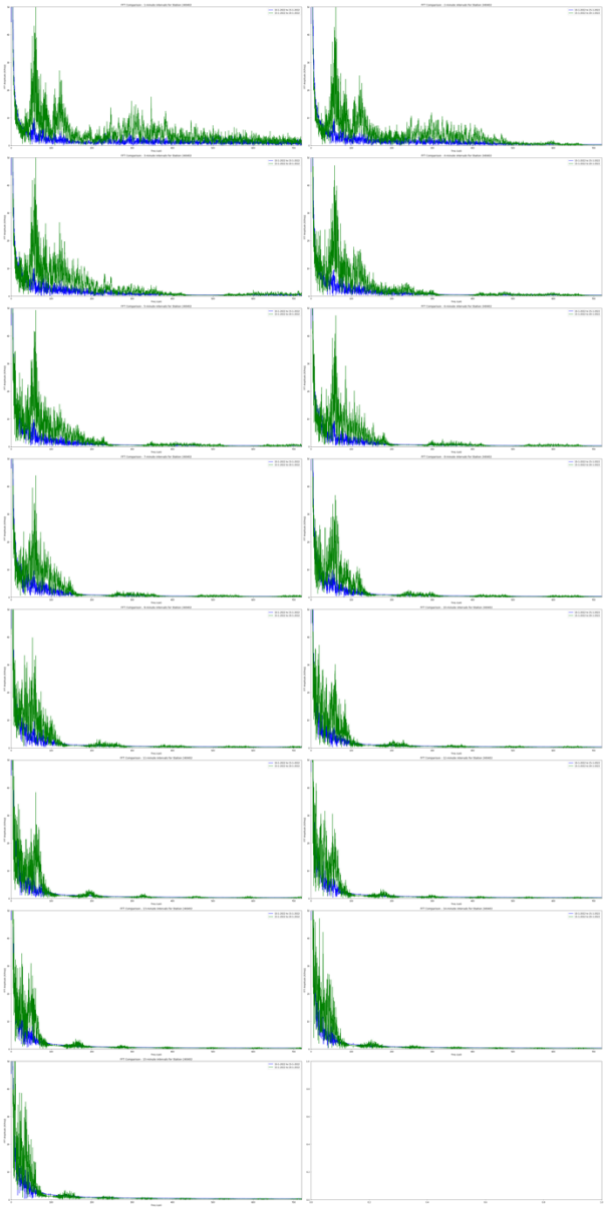

Figure 12 FFT plots comparing sea level frequencies for 5 days before (Blue), 5 days after (Green) the violent eruption for Station 240402, recorded from 1-minute to 15-minute intervals.